

Original Article

Inhibitory effects of hesperetin on Nav1.5 channels stably expressed in HEK 293 cells and on the voltage-gated cardiac sodium current in human atrial myocytes

Huan WANG^{1, #}, Hong-fei WANG^{2, #}, Hao ZHANG², Chen WANG¹, Yu-fang CHEN¹, Rong MA¹, Ji-zhou XIANG¹, Xin-ling DU², Qiang TANG^{1, *}

¹Department of Pharmacology, School of Basic Medicine, Tongji Medical College, Huazhong University of Science and Technology, Wuhan 430030, China; ²Department of Cardiovascular Surgery, Union Hospital, Tongji Medical College, Huazhong University of Science and Technology, Wuhan 430022, China

Aim: Voltage-gated sodium channels composed of a pore-forming α subunit and auxiliary β subunits are responsible for the upstroke of the action potential in cardiac myocytes. The pore-forming subunit of the cardiac sodium channel Nav1.5, which is encoded by SCN5A, is the main ion channel that conducts the voltage-gated cardiac sodium current (I_{Na}) in cardiac cells. The current study sought to investigate the inhibitory effects of hesperetin on human cardiac Nav1.5 channels stably expressed in human embryonic kidney 293 (HEK 293) cells and on the voltage-gated cardiac sodium current (I_{Na}) in human atrial myocytes.

Methods: The effects of hesperetin on human cardiac Nav1.5 channels expressed in HEK 293 cells and on cardiac Na^+ currents in human atrial myocytes were examined through whole-cell patch-clamp techniques.

Results: Nav1.5 currents were potently and reversibly suppressed in a concentration- and voltage-dependent manner by hesperetin, which exhibited an IC_{50} of 62.99 $\mu\text{mol/L}$. Hesperetin significantly and negatively shifted the voltage-dependent activation and inactivation curves. Hesperetin also markedly decelerated Nav1.5 current inactivation and slowed the recovery from Nav1.5 channel inactivation. The hesperetin-dependent blockage of Nav1.5 currents was frequency-dependent. Hesperetin also potently and reversibly inhibited Na^+ current (I_{Na}) in human atrial myocytes, consistently with its effects on Nav1.5 currents in HEK 293 cells.

Conclusion: Hesperetin is a potent inhibitor of I_{Na} in human atrial myocytes and Nav1.5 channels expressed in human embryonic kidney 293 cells. Hesperetin probably functions by blocking the open state and the inactivated state of these channels.

Keywords: hesperetin; Nav1.5 channel; voltage-gated cardiac sodium current (I_{Na}); whole-cell patch-clamp; HEK 293 cells; human atrial myocytes; cardiac arrhythmia

Acta Pharmacologica Sinica (2016) 37: 1563–1573; doi: 10.1038/aps.2016.97; published online Oct 3 2016

Introduction

Voltage-gated sodium channels (VGSCs) generate the upstroke of the action potential and regulate its propagation in various excitable cells^[1, 2]. They are composed of a pore-forming α subunit and one or two auxiliary β subunits^[3]. Of the nine VGSC α subunits (Nav1.1–1.9)^[4], Nav1.5, which is encoded by SCN5A^[5], is the most prominent sodium channel in the heart. It is well known that SCN5A-mediated sodium

currents are responsible for the rapid upstroke at the beginning of the cardiac action potential and that mutations or malfunctions in SCN5A-encoded Nav1.5 channels cause various arrhythmia-inducing conditions, such as type 3 long QT syndrome (LQTS3)^[6], Brugada syndrome (Brs)^[7], and sick sinus syndrome^[8]. It has been reported that blocking atrial Nav1.5 channels may be a useful antiarrhythmic strategy for treating atrial fibrillation^[9].

Hesperetin is found primarily in the young fruit of rutaceae citrus, which is increasingly being consumed in Western societies. Hesperetin is also found in orange juice at concentrations up to 720 mmol/L ^[10]. Epidemiological studies have shown that increased daily hesperetin intake reduces human mortal-

[#] These authors contributed equally to this work.

^{*} To whom correspondence should be addressed.

E-mail tangqiang_tjmu@hust.edu.cn

Received 2016-03-21 Accepted 2016-07-31

ity from cardiovascular diseases, lung cancer and asthma^[11]. Accumulating studies demonstrate that hesperetin is effective in treating many disorders because it exerts a wide range of biological effects, including vasorelaxation effects^[12], antioxidant effects^[13], neuroprotective effects^[14], anti-inflammatory effects^[15], antiviral effects and cholesterol-lowering effects^[16]. However, reports on the effects of hesperetin on ion channels are sparse. Recently, a report has described the inhibitory effects of hesperetin (IC₅₀ value of 267.4±26.5 μmol/L) on delayed rectifier potassium currents (I_{Kr}), which are encoded by the human ether-a-go-go-related gene (hERG)^[17]. Our previous study has also shown that hesperetin inhibits Kv1.5 channels^[18].

Until now, little attention has been paid to the relationship between hesperetin and Nav1.5 channels. In this study, we sought to investigate the pharmacologic effects of hesperetin on Nav1.5 channels expressed in HEK 293 cells and on voltage-gated cardiac sodium current (I_{Na}) in human atrial myocytes by using the whole-cell patch-clamp technique.

Materials and methods

Cell culture

Human cardiac Nav1.5 channels were stably expressed in HEK 293 cells, which were kindly provided by Prof Gui-Rong LI (University of Hong Kong). The cells were cultured in Dulbecco's modified Eagle's medium (DMEM, HyClone, Logan, UT, USA) containing 500 μg/mL G418 (Sigma-Aldrich, St Louis, MO, USA) and 10% (*v/v*) fetal bovine serum (FBS, Gibco, Gaithersburg, MD, USA) in a humidified atmosphere at 37°C with 5% CO₂-enriched air. The cells were passaged every 2–3 d by using brief trypsin treatments and were seeded on sterile glass cover slips for 24–48 h before the patch-clamp experiments.

Human atrial myocyte preparation

Human atrial cells were enzymatically dissociated as described previously^[19]. The method was approved by the Ethics Committee of Tongji Medical College, and the patients provided consent. Briefly, human atrial cells were enzymatically dissociated from the right atrial appendages of patients (*n*=5, 60.2±10.2 years of age) undergoing coronary artery bypass grafting and ablation for supraventricular tachyarrhythmias. The tissue samples were quickly immersed in O₂ 100%, Ca²⁺-free cardioplegic solution for transport to the laboratory after being removed from the atria, which were almost normal at the time of surgery. Atrial myocytes were enzymatically dissociated as described previously^[20]. Briefly, the atrial tissue samples were minced and gently bubbled with 100% O₂ in Ca²⁺-free Tyrode's solution for 15 min (5 min intervals in fresh solutions) and then incubated for 50 min in a similar solution containing 175 U/mL collagenase (type II, Sigma-Aldrich, St Louis, MO, USA), 1.2 U/mL proteinase (type XXIV, Sigma-Aldrich, St Louis, MO, USA) and 1 mg/mL bovine serum albumin (Sigma-Aldrich, St Louis, MO, USA). The tissue chunks were then re-incubated in a fresh enzyme solution with the same composition as that described above, but without

proteinase. After 25 min of incubation, the quantity and quality of the isolated cells were determined under a microscope at 5 min intervals. When the appearances of the cells seemed optimal, the chunks were suspended in a high K⁺ medium and gently triturated with a pipette to release individual myocytes. The isolated myocytes were maintained at room temperature in the above medium for at least 1 h before use.

Solutions and drugs

For $I_{Nav1.5}$ recording, we used a pipette solution containing the following (in mmol/L): 10.0 NaCl, 10.0 CsCl, 120.0 CsF, 1.0 MgCl₂, 1.0 CaCl₂, 10.0 EGTA, and 10.0 HEPES (pH adjusted to 7.4 with CsOH). We also used an extracellular bath solution containing the following (in mmol/L): 30.0 NaCl, 110.0 choline chloride, 5.0 CsCl, 1.2 MgCl₂, 2.0 CaCl₂, 10.0 HEPES, and 10.0 glucose (pH adjusted to 7.4 with NaOH). However, for I_{Na} recording in human atrial myocytes, we used a pipette solution containing the following (in mmol/L): 5 NaCl, 130 CsCl, 1 MgCl₂, 10 HEPES, 5 Cs-EGTA, 5 MgATP, and 0.1 GTP (pH adjusted to 7.2 with CsOH). The extracellular bath solution contained the following (in mmol/L): 140 NaCl, 1 MgCl₂, 10 glucose, 10 HEPES, 1.0 CaCl₂, and 1.0 CoCl (pH adjusted to 7.3 with CsOH). The Ca²⁺-free cardioplegic solution for tissue transport contained the following (in mmol/L): 10 taurine, 10 KH₂PO₄, 5 adenosine, 8 MgSO₄, 100 mannitol, 10 HEPES, and 140 glucose (pH adjusted to 7.3 with KOH). The high K⁺ medium contained the following (in mmol/L): 10 KCl, 120 K-glutamate, 10 taurine, 10 mannitol, 1.8 MgSO₄, 10 KH₂PO₄, 10 HEPES, 0.5 EGTA, and 20 glucose (pH adjusted to 7.3 with KOH). The standardized Tyrode's solution without Ca²⁺ included the following (in mmol/L): 140 NaCl, 5.4 KCl, 1.0 MgCl₂, 0.33 NaH₂PO₄, 5.0 HEPES, and 10.0 glucose (pH adjusted to 7.3–7.4 with NaOH). Hesperetin (purity ≥98%, as measured by HPLC) was purchased from Sigma-Aldrich and dissolved in dimethyl sulfoxide (DMSO) to produce a 1 mol/L stock solution. The stock solution was stored at -20°C and then deliquated with the bath solution to obtain the desired concentration. The concentration of DMSO in the final deliquation was less than 0.1% and had no effect on Nav1.5 currents.

Patch-clamp recording

We adopted the standard whole-cell patch-clamp technique to record sodium currents. For $I_{Nav1.5}$ recording, cells on cover slips were transferred to a continuously perfused recording chamber mounted on the stage of an inverted microscope and perfused with 10 mL of bath solution at a rate of about 1 mL/min for electrophysiological recording. Glass pipettes (1.5 mm diameter) were pulled with a two-stage microelectrode puller (PC-10, Narishige, Japan), and the resistance of the pipettes ranged from 2–4 MΩ when they were filled with the internal solution and immersed in the bath solution. For I_{Na} recording in human atrial myocytes, the solution containing the isolated cells was dropped in an open perfusion chamber (1 mL) mounted on the stage of an inverted microscope. The myocytes were allowed to adhere to the bottom of the cham-

ber for 10–15 min and were then superfused with bath solution at a rate of 2–3 mL/min. The resistance of the pipettes ranged from 2–3 M Ω when they were filled with the internal solution. Only quiescent rod-shaped cells showing clear cross-striations were used. Membrane currents were recorded with an EPC-10 amplifier and Pulse software (HEKA Elektronik, Lambrecht, Germany) at room temperature (22–24 °C). The liquid junction potentials between the pipette and bath solutions were compensated for before the pipette touched the cell. After obtaining a gigaohm seal, we ruptured the membrane via gentle suctioning to form the whole-cell configuration. The current signal was filtered at 3 kHz and sampled at 10 kHz. The whole-cell capacitance and resistance were compensated for, and the leak currents were subtracted. Currents were recorded 5 min after the whole-cell patch-clamp configuration was achieved.

Statistical analysis

Data analysis was performed using Pulsefit (HEKA) and Clampfit 10.0 (Molecular Devices). Nonlinear curve fitting was performed using SigmaPlot 11.0 (SPSS Science, Chicago, IL, USA). Values are presented as the mean \pm SEM. ANOVA was used to assess the statistical significance of the differences among multiple groups, and paired Student's *t*-tests were used to evaluate the differences between two groups. $P < 0.05$ was considered to be statistically significant.

Results

Hesperetin blocks Nav1.5 current in a concentration-dependent manner

Figure 1A shows the original representative traces of the Nav1.5 currents expressed in HEK 293 cell lines under control conditions or in the presence of hesperetin at concentrations of 10, 30, 100, and 300 μ mol/L. The inhibitory effect of hesperetin on Nav1.5 current amplitudes was concentration-dependent, and a maximum 49.25% reduction in Nav1.5 current amplitude was achieved at a concentration of 300 μ mol/L hesperetin. Fractional blockage was plotted against the corresponding concentrations of hesperetin ($n=7-8$ for each concentration) in a concentration-response curve, as shown in Figure 1B. The curve was well fitted by the Hill equation:

$$B (\%) = 100 / [1 + (IC_{50} / [D])^n] \quad (1)$$

where $B (\%)$ is the fractional blockage percentage change in Nav1.5 current amplitude at a given hesperetin concentration $[D]$, IC_{50} is the concentration at which hesperetin exerts 50% of its maximum effect, and n is the Hill coefficient. The IC_{50} of hesperetin was 62.99 μ mol/L, and the Hill coefficient (n) was 1.33.

Hesperetin blocks Nav1.5 current in a voltage-dependent manner

Current-voltage (*I-V*) relationships were studied to estimate the voltage dependence of the inhibitory effects of hesperetin on Nav1.5 channels. Figure 2A shows sample traces of the original currents to illustrate the inhibition of Nav1.5 by hesperetin. Hesperetin slightly decreased Nav1.5 currents

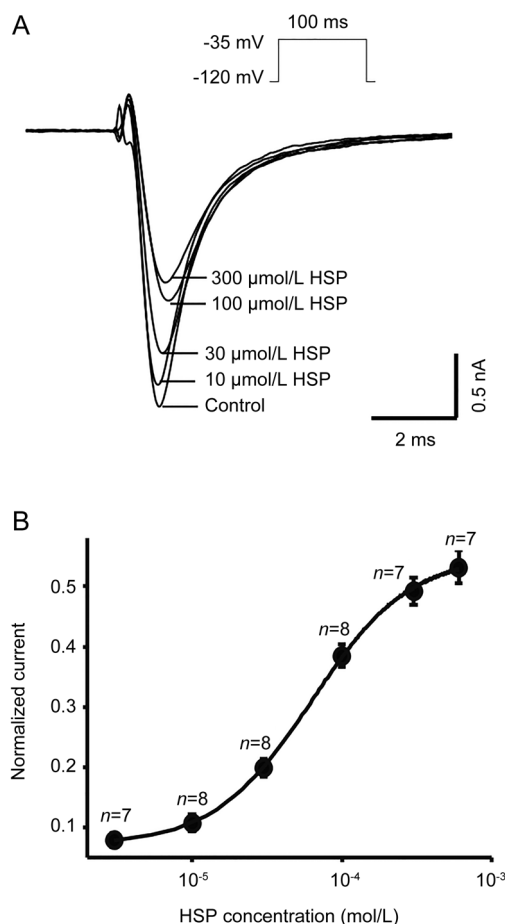


Figure 1. Hesperetin-mediated concentration-dependent blockage of Nav1.5 channels expressed in HEK 293 cells. (A) Original typical Nav1.5 currents recorded at -35 mV were elicited by application of 100-ms pulses causing depolarization from a holding potential of -120 mV to potentials ranging from -100 to +55 mV in the absence or presence of 10, 30, 100, or 300 μ mol/L hesperetin. (B) The summarized data show the concentration-response curve for hesperetin-mediated Nav1.5 current inhibition. Nav1.5 currents were measured during 100-ms depolarizing pulses of -35 mV. The plots indicate the percentages of Nav1.5 current blockage induced by 3, 10, 30, 100, 300, or 600 μ mol/L hesperetin. The normalized data were fitted with the Hill equation ($n=7-8$ for each concentration). Data are expressed as the mean \pm SEM. HSP indicates hesperetin.

at a concentration of 30 μ mol/L and substantially depressed Nav1.5 currents at a concentration of 100 μ mol/L. After a 10-min washout period, the effects of hesperetin on Nav1.5 currents was partially reversed. The *I-V* relationship curves pertaining to Nav1.5 currents were constructed in Figure 2B by plotting the amplitudes of the Nav1.5 currents against test pulse potentials ($n=9$, $P < 0.05$). Current inhibition was observed at all activating test potentials, thus suggesting that hesperetin-induced current blockage occurred over the entire potential activation range. Plotting the inhibition percentage against the test potential (Figure 2C) showed that hesperetin produced voltage-dependent inhibition between -45 and -30

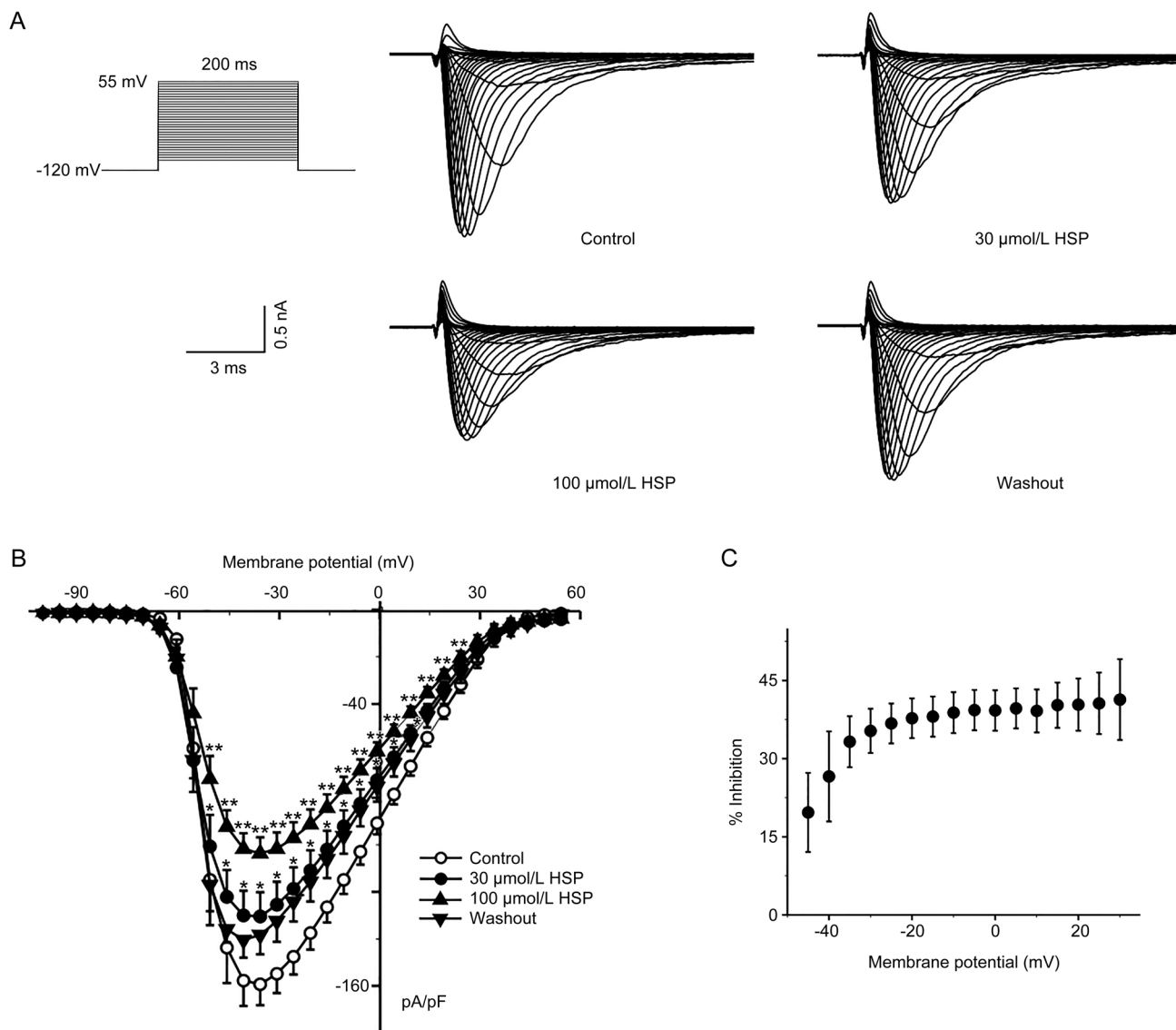


Figure 2. Hesperetin-mediated voltage-dependent Nav1.5 current inhibition. (A) Voltage-dependent Nav1.5 currents evoked by 200-ms pulses causing depolarization (increasing in steps of 5 mV every 1 s) from a holding potential of -120 mV to potentials ranging from -100 to +55 mV were recorded in a representative cell. (B) The summarized data show the Nav1.5 current-voltage (I - V) relationships before and after the application of 30 or 100 μmol/L hesperetin and washout ($n=9$). (C) The current inhibition percentage induced by the application of 100 μmol/L hesperetin is plotted against the membrane potential. Data are expressed as the mean \pm SEM. * $P<0.05$, ** $P<0.01$ vs control. HSP: hesperetin.

mV; the inhibition increased from 19.68% \pm 7.6% at -45 mV to 35.34% \pm 4.24% at -30 mV (Figure 2C, $n=8$, $P<0.05$) but increased only slightly from 35.33% \pm 4.2% at -30 mV to 41.34% \pm 7.7% at +30 mV (Figure 2C, $n=8$, $P=NS$). These results suggest that hesperetin-mediated Nav1.5 channel inhibition is dependent on these channels being in their open state.

Effects of hesperetin on steady-state Nav1.5 channel activation

The original traces of the voltage dependence of steady-state Nav1.5 channel activation in the absence or presence of hesperetin are shown in Figure 3A. The summarized data pertaining to Nav1.5 channel activation were fitted by the Boltzmann equation:

$$y=1/[1+\exp[(V-V_{1/2})/k]] \quad (2)$$

to form a conductance-voltage curve. A hyperpolarization shift of the steady-state activation curve was observed after 100 μmol/L hesperetin treatment. The midpoints of the channel activation values ($V_{1/2}$) were -47.83 \pm 2.1 mV in control cells and -54.45 \pm 1.9 mV in cells treated with 100 μmol/L hesperetin ($n=8$, $P<0.05$). The slope factors were 3.53 \pm 0.45 in control cells and 4.13 \pm 0.38 in cells treated with 100 μmol/L HSP ($n=8$, $P=NS$). These results suggested that hesperetin significantly shifted voltage-dependent channel opening to more hyperpolarized potentials.

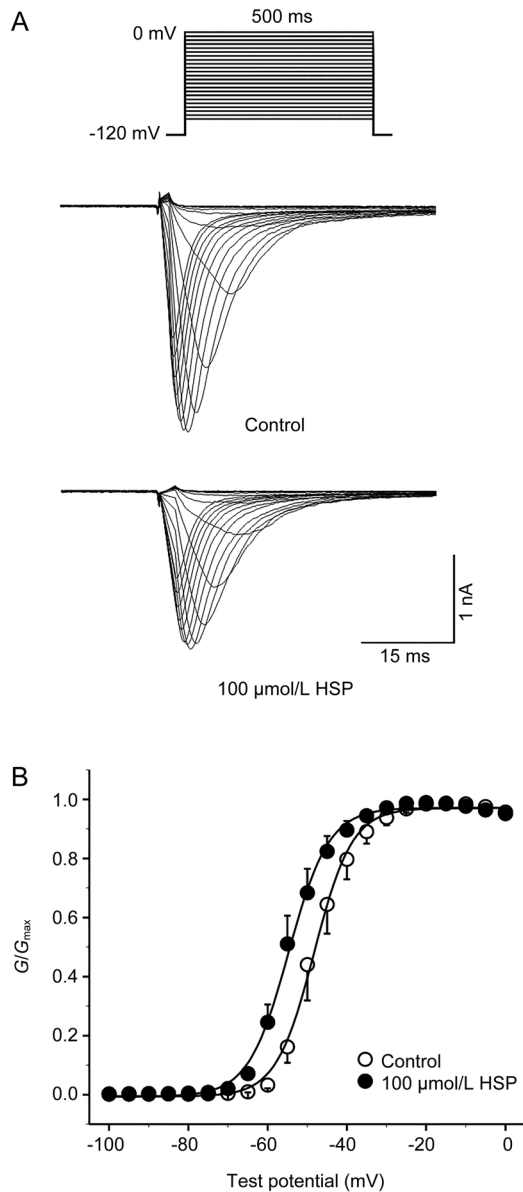


Figure 3. Effects of hesperetin on the steady-state activation of Nav1.5 channels expressed in HEK 293 cells. (A) Representative traces showing the steady-state activation of Nav1.5 currents that were triggered by 500-ms pulses causing depolarization (increasing in steps of 5 mV every 1 s) from a holding potential of -120 mV to potentials ranging from -100 to 0 mV in the absence or presence of 100 μmol/L hesperetin. (B) G/G_{\max} curves representing the steady-state activation of Nav1.5 currents in the absence or presence of 100 μmol/L hesperetin were fitted with the Boltzmann equation ($n=8$, $P<0.05$). Data are expressed as the mean \pm SEM.

Effects of hesperetin on steady-state Nav1.5 channel inactivation

Figure 4A shows the representative original traces of the voltage dependence of steady-state Nav1.5 channel inactivation in the absence or presence of 100 μmol/L hesperetin, which was evaluated by using a conventional double-pulse protocol, as shown in Figure 4A. Normalized data obtained under control

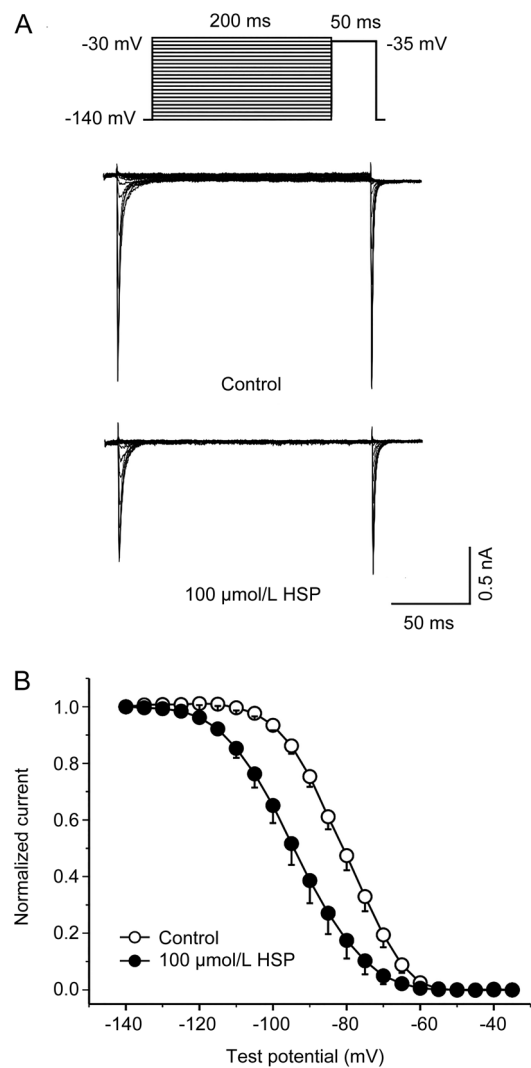


Figure 4. Effects of hesperetin on steady-state Nav1.5 channel inactivation. (A) Representative traces showing the steady-state inactivation of Nav1.5 currents. These traces were obtained using 200-ms pulses causing depolarization increasing in steps of 5 mV from a holding potential of -140 mV to a potential of -30 mV, followed by 50-ms pulses causing depolarization increasing at 5 s intervals from a holding potential of -140 mV to -35 mV. (B) The steady-state Nav1.5 current inactivation curves were fitted to the Boltzmann equation. The plots represent normalized mean currents during the test pulse as a function of the conditioning potential ($n=9$, $P<0.01$). Data are expressed as the mean \pm SEM.

conditions and those obtained after hesperetin exposure were plotted against the test membrane potential to illustrate the effects of hesperetin on the inactivation curve (Figure 4B). The curves were well fitted with the Boltzmann equation:

$$(I-I_0)/(I_{\max}-I_0)=a/[1+\exp(V-V_{1/2})/k] \quad (3)$$

Hesperetin had little effect on the inactivation slope factor but elicited a significant negative shift with respect to steady-state Nav1.5 channel inactivation. As shown in Figure 4B, the midpoint of the channel inactivation value ($V_{1/2}$) of control

cells was -80.8 ± 1.65 mV, whereas that of cells treated with $100 \mu\text{mol/L}$ hesperetin was -93.8 ± 2.88 mV ($n=9$, $P<0.01$). The slope factor (k) was 7.45 ± 0.16 for control cells and 7.7 ± 0.17 for cells treated with $100 \mu\text{mol/L}$ hesperetin ($n=9$, $P=\text{NS}$).

Effects of hesperetin on the time constants of Nav1.5 channel inactivation

The time constants of Nav1.5 channel inactivation were investigated and were found to be well-fitted with the mono-exponential function, as shown in Figure 5A ($n=9$). The inactivation time constants were significantly increased by $100 \mu\text{mol/L}$ hesperetin treatment at test potentials ranging from -45 mV to -10 mV. The inactivation time constants were increased from 1.81 ± 0.19 ms to 2.13 ± 0.14 ms at -45 mV in hesperetin-treated cells (Figure 5B, $n=9$, $P<0.05$ vs control). These results suggested that hesperetin slows time-dependent Nav1.5 channel inactivation.

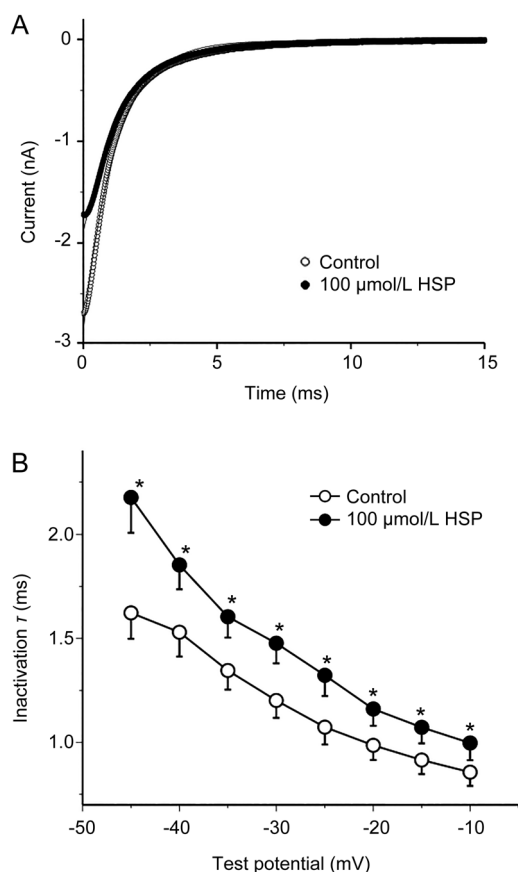


Figure 5. Effects of hesperetin on the time constants of Nav1.5 channel inactivation. (A) Representative traces showing the original plots of Nav1.5 current inactivation and the curve fitted by a mono-exponential function before and after $100 \mu\text{mol/L}$ hesperetin treatment at a potential of -35 mV ($n=9$). (B) The time constant (τ) of inactivation (from the peak to the end of the depolarizing pulse) measured by fitting the single-exponential function is plotted against different voltages. Mean \pm SEM. $n=9$. $*P<0.05$ vs control. HSP: hesperetin.

Hesperetin-mediated frequency-dependent Nav1.5 channel blockage

Hesperetin-mediated frequency-dependent Nav1.5 channel blockage was evaluated with twenty duplicate 50-ms pulses that caused depolarization from a holding potential of -120 mV to a potential of -35 mV at frequencies of 2, 5, and 10 Hz (Figure 6A). The amplitudes of the Nav1.5 currents were slightly reduced after the twenty depolarizing pulses (Figure 6B, $n=11$, $P<0.01$). If the blockage percentage elicited by the first depolarizing pulse was considered to be a tonic block, frequency-dependent inhibition could be identified on the basis of the reductions in the amplitudes of Nav1.5 currents elicited by subsequent pulses. In the presence of $100 \mu\text{mol/L}$ hesperetin, the Nav1.5 channel tonic block percentages were $35.01\% \pm 3.5\%$ at 2 Hz, $35.13\% \pm 4.5\%$ at 5 Hz, and $35.99\% \pm 4.7\%$ at 10 Hz ($n=8$, $P=\text{NS}$), and frequency-dependent inhibition increased from $36.17\% \pm 4.2\%$ at 2 Hz ($n=8$, $P=\text{NS}$) to $40.23\% \pm 4.8\%$ at 5 Hz ($n=8$, $P<0.05$) to $49.25\% \pm 6\%$ at 10 Hz ($n=8$, $P<0.01$) (Figure 6C). These results showed that hesperetin induces use-dependent Nav1.5 channel blockage.

Effects of hesperetin on recovery from Nav1.5 channel inactivation

Recovery from inactivation at repolarizing potentials was assessed by using a double-pulse protocol. Figure 7A shows the representative original tracings of the recovery from Nav1.5 channel inactivation in the absence or presence of hesperetin. Recovery from inactivation was represented by the ratio of the test amplitude to the conditioning pulses. The time course for recovery was well fitted with the double-exponential function:

$$y = y_0 + A_1[1 - \exp(-t/\tau_1)] + A_2[1 - \exp(-t/\tau_2)] \quad (4)$$

The fast time constant (τ_1) was 8.62 ± 1.67 ms, and the slow time constant (τ_2) was 50.62 ± 10.5 ms in the absence of hesperetin (Figure 7B, $n=8$). Recovery from inactivation was slowed by $100 \mu\text{mol/L}$ HSP, the fast time constant (τ_1) was 27.21 ± 6.9 ms ($n=8$, $P<0.05$), and the slow time constant (τ_2) was 157.2 ± 25.61 ms ($n=8$, $P<0.01$). These results suggest that hesperetin significantly slows both the slow and fast components of the recovery from inactivation, thus indicating that hesperetin-binding channels require more time to recover from inactivation than non-binding channels.

Effects of hesperetin on I_{Na} in human atrial myocytes

The effects of hesperetin on I_{Na} in human atrial myocytes are illustrated in Figure 8. Figure 8A shows the representative voltage-dependent I_{Na} traces recorded in a human right atrial cell in the absence or presence of 30 and $100 \mu\text{mol/L}$ hesperetin and after washout. Hesperetin substantially inhibited I_{Na} at concentrations of 30 and $100 \mu\text{mol/L}$, and these effects were partly reversed after a 10-min drug washout. Figure 8B displays the I - V relation curves of the mean I_{Na} values ($n=5$) in the absence or presence of different concentrations of hesperetin. I_{Na} was significantly inhibited by hesperetin in a concentration-dependent manner. At -45 mV, I_{Na} was inhibited

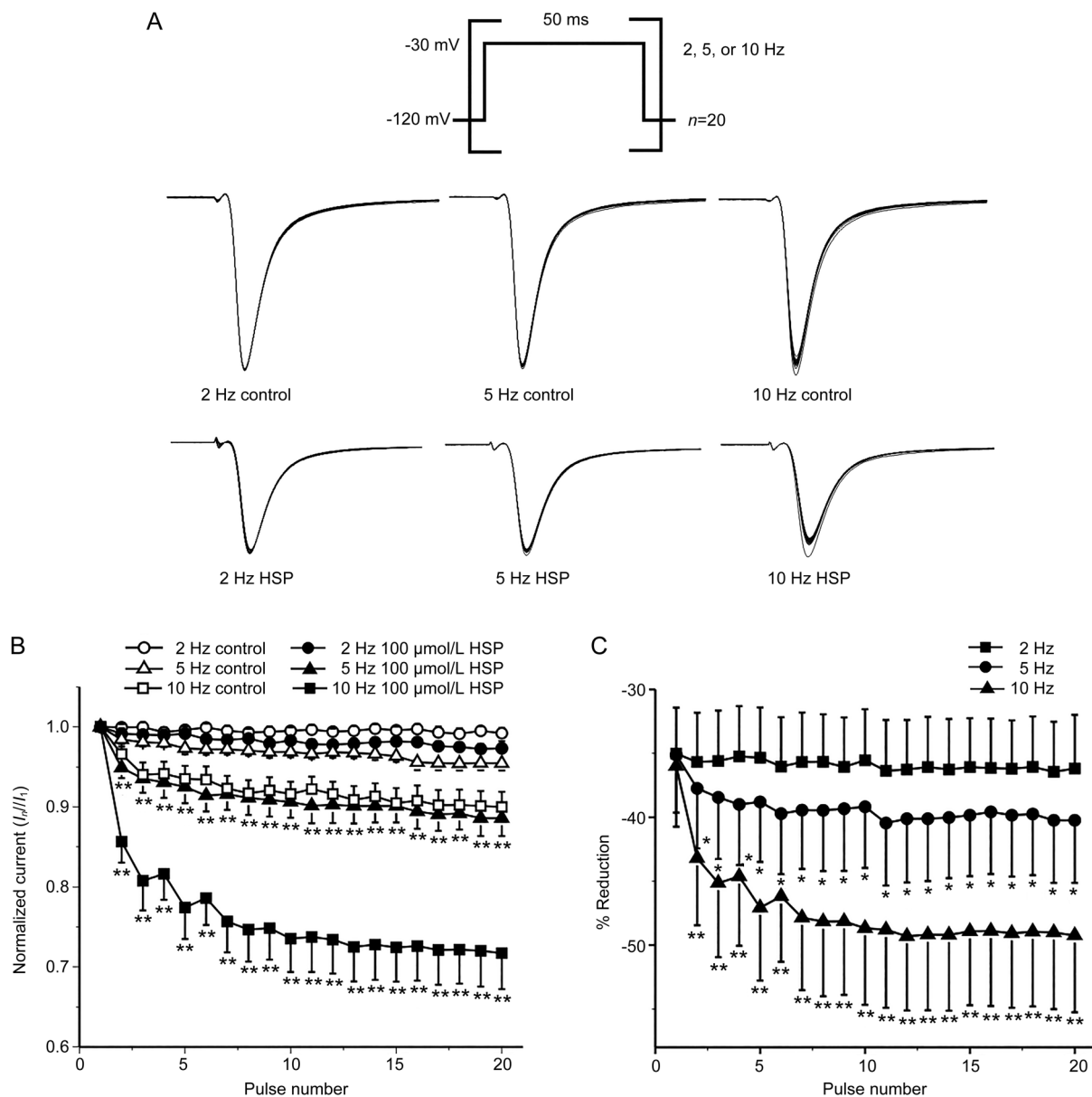


Figure 6. Hesperetin-mediated frequency-dependent Nav1.5 channel blockage. (A) Thirty repetitive 50-ms pulses causing depolarization from a holding potential of -120 mV to -30 mV were applied at three different frequencies, 2, 5, and 10 Hz, in the absence or presence of 100 μmol/L hesperetin. (B) The amplitudes of the currents achieved during each pulse were normalized to the amplitudes of the currents acquired during the first pulse and then plotted against pulse numbers (*n*=11). ***P*<0.01 vs corresponding control. (C) Hesperetin (100 μmol/L)-induced changes (%) in current amplitude are plotted against pulse numbers (*n*=8). Data are expressed as the mean±SEM. **P*<0.05, ***P*<0.01 vs 2 Hz. HSP: hesperetin.

ited by 12.43%±0.01% and 22.53%±0.04% (*n*=5, *P*<0.05) at concentrations of 30 and 100 μmol/L hesperetin, respectively, and was substantially recovered after washout. These results suggested that hesperetin significantly and reversibly inhibits I_{Na} in a concentration- and voltage-dependent manner. I_{Na} activation was fitted by the Boltzmann equation as described above to generate a conductance-voltage curve, as shown in Figure 8C. A hyperpolarization shift of the steady-state activation curve was observed after treatment with 100 μmol/L hesperetin. The midpoint of the channel activation value ($V_{1/2}$) was -60.49±1.45 mV in control cells and -67.48±2.47 mV in cells

treated with 100 μmol/L hesperetin (*n*=5, *P*<0.05). The slope factors were 0.12±0.04 in control cells and 0.15±0.04 in cells treated with 100 μmol/L HSP (*n*=5, *P*=NS). These results suggested that hesperetin significantly shifts voltage-dependent activation to more hyperpolarized potentials which were consistent with the results of the experiments on human cardiac Nav1.5 channels expressed in HEK 293 cells.

Discussion

The present work provides the first demonstration that hesperetin is a potent direct inhibitor of open Nav1.5 channels. The

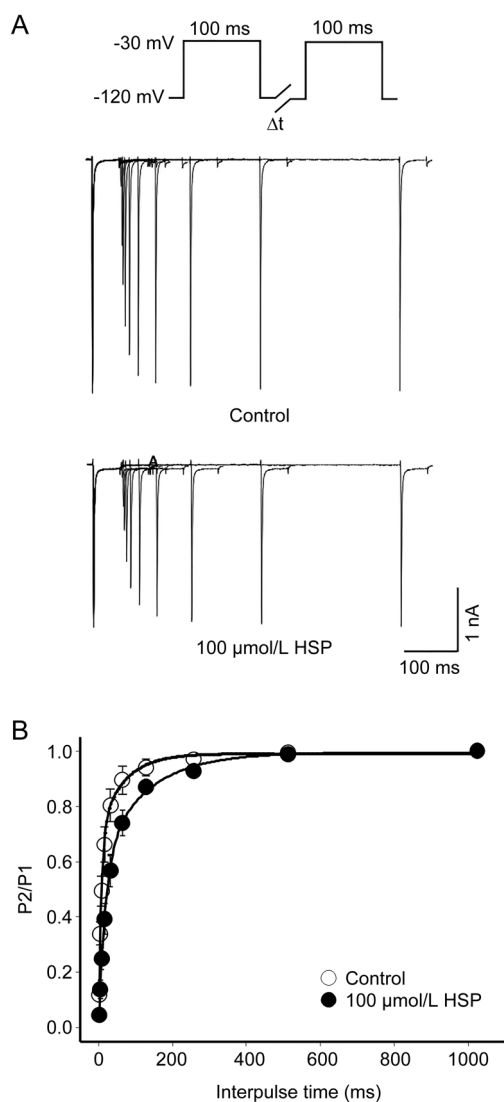


Figure 7. Effects of hesperetin on recovery from Nav1.5 channel inactivation. (A) Representative traces showing the recovery of Nav1.5 channels from inactivation evoked by the double-pulse protocol in the absence or presence of 100 $\mu\text{mol/L}$ hesperetin. The cells were depolarized from a holding potential of -120 mV to a potential of -30 mV for 50-ms (P1) and then returned to the holding potential for a time interval ranging from 2 to 1200 ms before being depolarized by a second 50-ms pulse from -120 mV to -30 mV (P2). (B) The relative amplitudes of $I_{\text{Nav1.5}}$ (P2/P1) are plotted against the inter-pulse interval. The recovery curves were well fitted with a double-exponential function. Data are expressed as the mean \pm SEM. $n=8$. HSP: hesperetin.

following novel findings support this statement: (1) Nav1.5 currents were potently and reversibly blocked by hesperetin in a voltage- and concentration-dependent manner, (2) hesperetin significantly shifted both the steady-state activation curve and the steady-state inactivation curve of Nav1.5 currents in the negative direction, (3) hesperetin decelerated Nav1.5 channel inactivation and slowed Nav1.5 channel recovery from inactivation, (4) hesperetin-dependent Nav1.5 current block-

age is frequency-dependent, (5) hesperetin significantly and reversibly blocked I_{Na} in human atrial myocytes in a voltage- and concentration-dependent manner and shifted the steady-state activation curve of I_{Na} in a negative direction.

The current study suggests that hesperetin potently inhibits Nav1.5 currents in a concentration-dependent manner, exhibiting a half-maximal inhibitory concentration (IC_{50}) of 62.99 $\mu\text{mol/L}$. It has been reported that intragastric administration of 100 mg/kg hesperetin to rats induces hesperetin plasma concentrations as high as 20–30 $\mu\text{mol/L}$ ^[21]. The IC_{50} value of hesperetin required to affect Nav1.5 currents is twice the plasma concentration in rats; however, hesperetin is a highly lipid soluble compound that can accumulate at higher concentrations in tissues than in plasma^[22]. Therefore, the local concentrations required to block Nav1.5 currents may be achieved in clinical settings.

Pore blockers usually cause use-dependent channel blockage. Frequency-dependent blockage is the most common type of use-dependent blockage reported to be induced by many drugs, such as A-803467^[5], ranolazine^[23], mexiletine and propafenone^[24], all of which block open sodium channels. Hesperetin-mediated Nav1.5 channel blockage is also frequency-dependent, thus indicating that higher frequencies increase the total amount of time that Nav1.5 channels spend in their open state, in which they can be bound by hesperetin, thereby leading to enhanced blockage, and that hesperetin preferentially binds to Nav1.5 channels when they are in their open state, as do mexiletine and lidocaine^[25]. This hypothesis was confirmed by a study demonstrating the strongly voltage-dependent blockage of open Nav1.5 channels induced by quinidine^[26]. Hesperetin also shifted the maximum conductance and the activation curve toward negative potentials, thus indicating that the effects of hesperetin are voltage dependent, as are those of other open channel blockers, such as disopyramide and mibefradil^[27, 28]. All these findings strongly suggested that hesperetin blocks open Nav1.5 channels.

The current study also showed that hesperetin inhibits Nav1.5 currents not only by shifting the voltage dependence of steady-state inactivation in a hyperpolarizing direction but also by slowing Nav1.5 channel inactivation and recovery from inactivation, thus suggesting that hesperetin binds not only to open Nav1.5 channels but also to inactive Nav1.5 channels, as do other open channel blockers. This finding may indicate that the Nav1.5 channels have a window region in which the steady-state activation curve and inactivation curve overlap. Similar phenomena have also been observed with respect to the effects of other open channel blockers on other channels; for example, neferine interacts with both open and inactive Kv4.3 channels^[29], BAPTA-AM interacts with both open and inactive hERG channels^[30], and carvedilol and pergolide interact with both open and inactive Kv1.5 channels^[31, 32].

Mammalian species express nine functional voltage-gated Na^+ channels. Of these, the cardiac-specific isoform Nav1.5 is relatively resistant to the neurotoxin tetrodotoxin (TTX)^[33]. In the present study, the inhibitory effects of hesperetin on Nav1.5 current amplitudes were concentration-dependent,

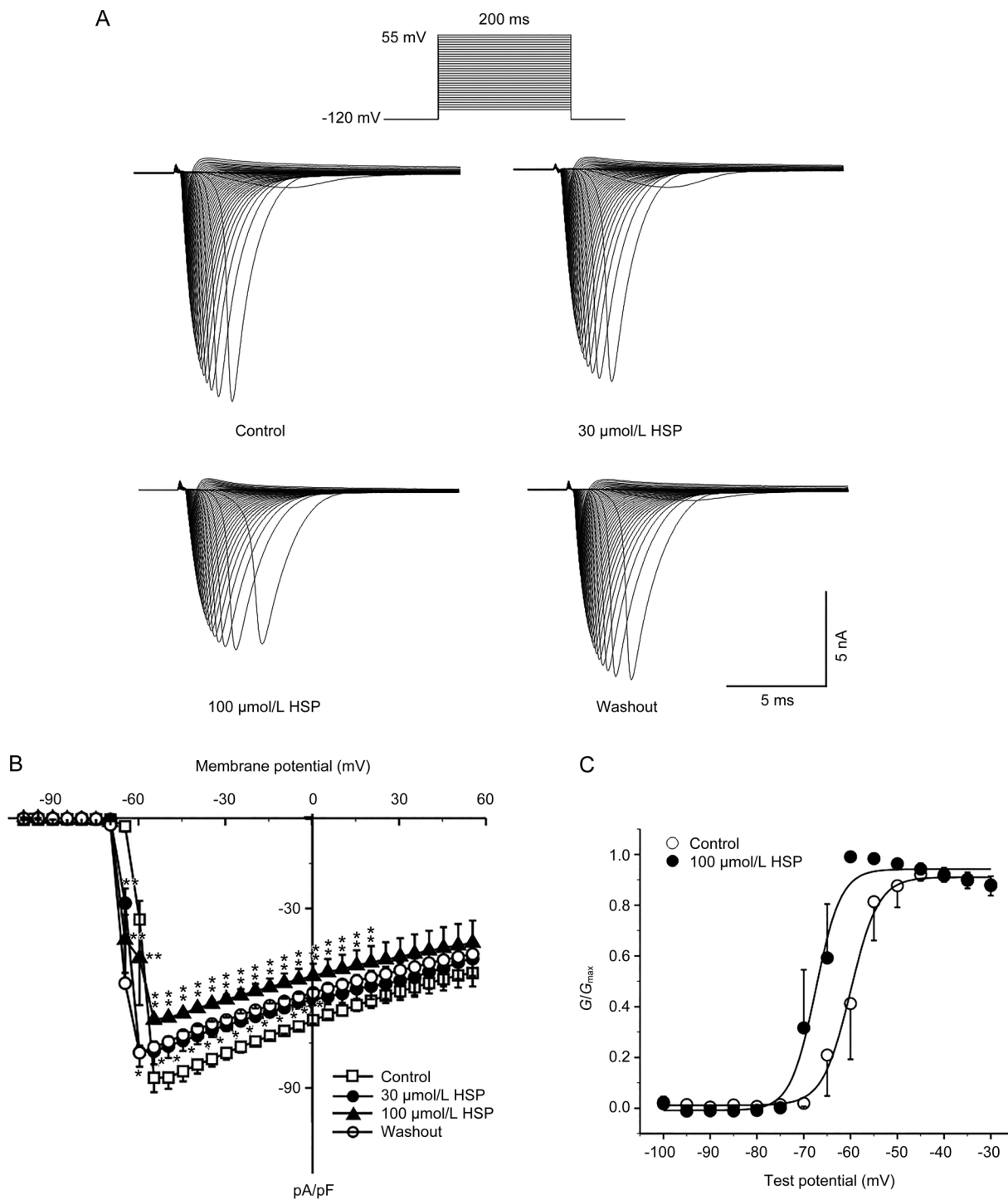


Figure 8. Effects of hesperetin on I_{Na} in human atrial myocytes. (A) Voltage-dependent I_{Na} traces showing 200-ms pulses causing depolarization (increasing in steps of 5 mV every 1 s) from a holding potential of -120 mV to potentials ranging from -100 to +55 mV in a representative atrial myocyte. (B) I_{Na} I - V relationships in the absence or presence of 30 and 100 $\mu\text{mol/L}$ hesperetin and after washout are shown. (C) G/G_{max} curves representing steady-state I_{Na} current activation in the absence or presence of 100 $\mu\text{mol/L}$ hesperetin were fitted with the Boltzmann equation. Data are expressed as the mean \pm SEM. $n=5$. * $P<0.05$, ** $P<0.01$ vs control.

and hesperetin induced with $19.92\pm 0.01\%$ and $38.51\pm 0.02\%$ reductions in Nav1.5 current amplitudes at concentrations of 30 and 100 $\mu\text{mol/L}$. Functional studies have shown that

the TTX-nosensitive (Nav1.5) isoform accounts for up to 73% of total sodium currents in the human atrium^[34]. I_{Na} in human atrial myocytes was inhibited by $12.43\pm 0.01\%$ and

22.53%±0.04% by treatment with 30 and 100 μmol/L hesperetin, respectively, at -45 mV, findings consistent with the effects of hesperetin on Nav1.5 channels in HEK 293 cells. Furthermore, Nav1.5 channels activate at more negative potentials than do TTX-sensitive channels, and test potentials of -60 mV have been shown to activate Nav1.5 channels but not TTX-sensitive channels^[35]. These results suggest that the effects of hesperetin on I_{Na} are primarily mediated via Nav1.5 channel blockage.

In the current study, the steady-state activation curve of I_{Na} in human atrial myocytes was shifted in a negative direction by hesperetin, which exerted similar effects on the steady-state activation curve of Nav1.5 channels in HEK 293 cells. However, the midpoint of the channel inactivation value ($V_{1/2}$) of the I_{Na} steady-state activation curve in human atrial myocytes was more negative than that of the Nav1.5 channel steady-state activation curve in HEK 293 cells, which may have been caused by differences in the sodium concentrations of the extracellular bath solutions. Higher extracellular bath sodium concentrations shifted the I_{Na} steady-state activation curve in a negative direction in human atrial myocytes.

Many reports have documented that inherited or acquired sodium channel dysfunction resulting in excessive sodium conductance can lead to cardiac arrhythmias^[36], and therapeutic agents that inhibit sodium conductance, such as quinidine^[37], A-803467^[5], and lacosamide^[38], are widely used to manage these diseases^[24]. Nav1.5-mediated sodium currents are responsible for the rapid upstroke at the beginning of the cardiac action potential, and Na^+ channel blockers with potential- and frequency-dependent effects preferentially suppress atrial fibrillation because the high excitation rate induced by the disease promotes drug binding in atrial cells^[9]. Hesperetin potently inhibits the currents of Nav1.5, a protein encoded by SCN5A, and may therefore have potential as an anti-arrhythmic drug that can be used to treat atrial fibrillation. High hesperetin concentrations have been found in oranges and orange juice, whose consumption is increasing in Europe; thus, the potential beneficial effects exerted by hesperetin on cardiac electrophysiology *in vivo* warrant further investigation.

In conclusion, our results strongly indicate that hesperetin is a potent blocker of Nav1.5 channels and that it interacts with these channels when they are in their open and inactivated states.

Acknowledgements

We thank Dr Gui-rong LI (University of Hong Kong) for providing the HEK 293 cells stably expressing Nav1.5 channels.

Author contribution

Qiang TANG, Ji-zhou XIANG, and Xin-ling DU designed the study; Huan WANG, Hao ZHANG, Chen WANG, and Yu-fang CHEN performed the experiments; Huan WANG and Rong MA analyzed the data; Hong-fei WANG, Chen WANG, and Yu-fang CHEN provided the reagents and materials; and Huan WANG, Hong-fei WANG, and Qiang TANG wrote the paper.

References

- 1 Kleber AG, Rudy Y. Basic mechanisms of cardiac impulse propagation and associated arrhythmias. *Physiol Rev* 2004; 84: 431–88.
- 2 Catterall WA, Goldin AL, Waxman SG. International Union of Pharmacology. XLVII. Nomenclature and structure-function relationships of voltage-gated sodium channels. *Pharmacol Rev* 2005; 57: 397–409.
- 3 Catterall WA. From ionic currents to molecular mechanisms: the structure and function of voltage-gated sodium channels. *Neuron* 2000; 26: 13–25.
- 4 Goldin AL. Resurgence of sodium channel research. *Annu Rev Physiol* 2001; 63: 871–94.
- 5 Han Z, Jiang Y, Xiao F, Cao K, Wang DW. The effects of A-803467 on cardiac Nav1.5 channels. *Eur J Pharmacol* 2015; 754: 52–60.
- 6 Bennett PB, Yazawa K, Makita N, George AL Jr. Molecular mechanism for an inherited cardiac arrhythmia. *Nature* 1995; 376: 683–5.
- 7 Priori SG, Wilde AA, Horie M, Cho Y, Behr ER, Berul C, et al. HRS/EHRA/APHS expert consensus statement on the diagnosis and management of patients with inherited primary arrhythmia syndromes: document endorsed by HRS, EHRA, and APHS in May 2013 and by ACCF, AHA, PACES, and AEPC in June 2013. *Heart Rhythm* 2013; 10: 1932–63.
- 8 Bolli R. The new circulation research: a manifesto. *Circ Res* 2010; 106: 216–26.
- 9 Ravens U, Poulet C, Wettwer E, Knaut M. Atrial selectivity of antiarrhythmic drugs. *J Physiol* 2013; 591: 4087–97.
- 10 Erlund I, Merinne E, Alfthan G, Aro A. Plasma kinetics and urinary excretion of the flavanones naringenin and hesperetin in humans after ingestion of orange juice and grapefruit juice. *J Nutr* 2001; 131: 235–41.
- 11 Knekt P, Kumpulainen J, Jarvinen R, Rissanen H, Heliovaara M, Reunanen A, et al. Flavonoid intake and risk of chronic diseases. *Am J Clin Nutr* 2002; 76: 560–8.
- 12 Calderone V, Chericoni S, Martinelli C, Testai L, Nardi A, Morelli I, et al. Vasorelaxing effects of flavonoids: investigation on the possible involvement of potassium channels. *Naunyn-Schmiedeberg's Arch Pharmacol* 2004; 370: 290–8.
- 13 Kumar B, Gupta SK, Srinivasan BP, Nag TC, Srivastava S, Saxena R, et al. Hesperetin rescues retinal oxidative stress, neuroinflammation and apoptosis in diabetic rats. *Microvasc Res* 2013; 87: 65–74.
- 14 Cho J. Antioxidant and neuroprotective effects of hesperidin and its aglycone hesperetin. *Arch Pharm Res* 2006; 29: 699–706.
- 15 Emim JA, Oliveira AB, Lapa AJ. Pharmacological evaluation of the anti-inflammatory activity of a citrus bioflavonoid, hesperidin, and the isoflavonoids, dauricin and claussequinone, in rats and mice. *J Pharm Pharmacol* 1994; 46: 118–22.
- 16 Garg A, Garg S, Zaneveld LJ, Singla AK. Chemistry and pharmacology of the *Citrus* bioflavonoid hesperidin. *Phytother Res* 2001; 15: 655–69.
- 17 Scholz EP, Zitron E, Kiesecker C, Thomas D, Kathofer S, Kreuzer J, et al. Orange flavonoid hesperetin modulates cardiac hERG potassium channel via binding to amino acid F656. *Nutr Metab Cardiovasc Dis* 2007; 17: 666–75.
- 18 Wang H, Wang HF, Wang C, Chen YF, Ma R, Xiang JZ, et al. Inhibitory effects of hesperetin on Kv1.5 potassium channels stably expressed in HEK 293 cells and ultra-rapid delayed rectifier K^+ current in human atrial myocytes. *Eur J Pharmacol* 2016; 789: 98–108.
- 19 Li GR, Wang HB, Qin GW, Jin MW, Tang Q, Sun HY, et al. Acacetin, a natural flavone, selectively inhibits human atrial repolarization potassium currents and prevents atrial fibrillation in dogs. *Circulation* 2008; 117: 2449–57.
- 20 Benjamin EJ, Wolf PA, D'Agostino RB, Silbershatz H, Kannel WB, Levy D.

- Impact of atrial fibrillation on the risk of death: the Framingham Heart Study. *Circulation* 1998; 98: 946–52.
- 21 Duffy SJ, Keaney JF Jr, Holbrook M, Gokce N, Swerdlow PL, Frei B, *et al*. Short- and long-term black tea consumption reverses endothelial dysfunction in patients with coronary artery disease. *Circulation* 2001; 104: 151–6.
- 22 Takumi H, Mukai R, Ishiduka S, Kometani T, Terao J. Tissue distribution of hesperetin in rats after a dietary intake. *Biosci Biotechnol Biochem* 2011; 75: 1608–10.
- 23 Sokolov S, Peters CH, Rajamani S, Ruben PC. Proton-dependent inhibition of the cardiac sodium channel Nav1.5 by ranolazine. *Front Pharmacol* 2013; 4: 78.
- 24 Pless SA, Galpin JD, Frankel A, Ahern CA. Molecular basis for class Ib anti-arrhythmic inhibition of cardiac sodium channels. *Nat Commun* 2011; 2: 351.
- 25 Wang Y, Mi J, Lu K, Lu Y, Wang K. Comparison of gating properties and use-dependent block of Nav1.5 and Nav1.7 channels by anti-arrhythmics mexiletine and lidocaine. *PLoS One* 2015; 10: e0128653.
- 26 Wang Z, Fermini B, Nattel S. Effects of flecainide, quinidine, and 4-aminopyridine on transient outward and ultrarapid delayed rectifier currents in human atrial myocytes. *J Pharmacol Exp Ther* 1995; 272: 184–96.
- 27 Arechiga IA, Barrio-Echavarria GF, Rodriguez-Menchaca AA, Moreno-Galindo EG, Decher N, Tristani-Firouzi M, *et al*. Kv1.5 open channel block by the antiarrhythmic drug disopyramide: molecular determinants of block. *J Pharmacol Sci* 2008; 108: 49–55.
- 28 Perchenet L, Clement-Chomienne O. Characterization of mibefradil block of the human heart delayed rectifier hKv1.5. *J Pharmacol Exp Ther* 2000; 295: 771–8.
- 29 Wang C, Chen YF, Quan XQ, Wang H, Zhang R, Xiao JH, *et al*. Effects of neferine on Kv4.3 channels expressed in HEK293 cells and *ex vivo* electrophysiology of rabbit hearts. *Acta Pharmacol Sin* 2015; 36: 1451–61.
- 30 Tang Q, Jin MW, Xiang JZ, Dong MQ, Sun HY, Lau CP, *et al*. The membrane permeable calcium chelator BAPTA-AM directly blocks human ether a-go-go-related gene potassium channels stably expressed in HEK 293 cells. *Biochem Pharmacol* 2007; 74: 1596–607.
- 31 Jeong I, Choi BH, Yoon SH, Hahn SJ. Carvedilol blocks the cloned cardiac Kv1.5 channels in a beta-adrenergic receptor-independent manner. *Biochem Pharmacol* 2012; 83: 497–505.
- 32 Jeong I, Choi BH, Hahn SJ. Pergolide block of the cloned Kv1.5 potassium channels. *Naunyn-Schmiedeberg's Arch Pharmacol* 2013; 386: 125–33.
- 33 Zimmer T, Haufe V, Blechschmidt S. Voltage-gated sodium channels in the mammalian heart. *Glob Cardiol Sci Practice* 2014; 2014: 449–63.
- 34 Kaufmann SG, Westenbroek RE, Maass AH, Lange V, Renner A, Wischmeyer E, *et al*. Distribution and function of sodium channel subtypes in human atrial myocardium. *J Mol Cell Cardiol* 2013; 61: 133–41.
- 35 Smith RD, Goldin AL. Functional analysis of the rat I sodium channel in xenopus oocytes. *J Neurosci* 1998; 18: 811–20.
- 36 Viswanathan PC, Balse JR. Inherited sodium channelopathies: a continuum of channel dysfunction. *Trends Cardiovasc Med* 2004; 14: 28–35.
- 37 Stokoe KS, Thomas G, Goddard CA, Colledge WH, Grace AA, Huang CL. Effects of flecainide and quinidine on arrhythmogenic properties of Scn5a+/Delta murine hearts modelling long QT syndrome 3. *J Physiol* 2007; 578: 69–84.
- 38 Wang GK, Wang SY. Block of human cardiac sodium channels by lacosamide: evidence for slow drug binding along the activation pathway. *Mol Pharmacol* 2014; 85: 692–702.